Bulletin of Biological and Allied Sciences Research
***ISSN:* 2521-0092**
www.bbasr.org
DOI: https://doi.org/10.64013/bbasr.v2026i1.134
*Bull. Biol. All. Sci. Res., Volume, **11**: 134*
Original Research Article ***Open Access***

ISOLATION AND CHARACTERIZATION OF INDIGENOUS SOIL BACTERIA FOR SUSTAINABLE SELF-HEALING CONCRETE VIA MICROBIALLY INDUCED CALCITE PRECIPITATION

JAMSHAID[1], SHIREEN F[2*], KHALIL MS[1], HABIB F[3], YILMAZ S[4], AZIZ A[1], KHAN S[5]

[1]Sarhad University of Science and Information Technology, Peshawar, Pakistan
[2]School of Allied Health Sciences, Iqra National University Peshawar, Pakistan
[3]School of Pharmacy, Medicine and Biomedical Sciences, University of Portsmouth, United Kingdom
[4]Department of Agricultural Biotechnology, Erciyes University, Kayseri, Turkey
[5]School of Resources and Environmental Engineering, East China University of Science and Technology, Shanghai, 200237, China
**Correspondence Author Email Address: farahshireen@inu.edu.pk; sarakhan17301@gmail.com*

(Received, 17th February 2026, Accepted 18th July 2026, Published 29th July 2026)

Abstract *Microbially Induced Calcite Precipitation (MICP) is a revolutionary bio-mineralization technology that has great potential for sustainable construction applications. The present study isolated, identified, characterized, and evaluated the potential calcium carbonate precipitation-producing positive bacteria from agricultural soils of Peshawar in Khyber Pakhtunkhwa, Pakistan, and their potential for concrete crack healing. Three bacterial isolates with the highest urease activity were isolated from three different agricultural soil samples: Bacillus cereus (580 U/mL, Day 4), Pseudomonas aeruginosa (525 U/mL, Day 6), and Staphylococcus aureus (515U/mL, Day 6). All isolates were identified by Gram staining, biochemical tests, and 16S rRNA sequencing. $CaCO_3$ precipitation was induced in vitro by introducing cultures to nutrient broth containing 3% urea and 24 mM $CaCl_2$ at pH 9.0. Physicochemical analysis of soil showed an alkaline reaction in pH (8.66–8.67), which is favorable for the growth of ureolytic bacteria, loamy to silt texture, and moisture content (29.33 to 31.51%). Scanning Electron Microscopy (SEM) characterization of precipitates showed the polymorphic crystal forms of $CaCO_3$, such as irregular cubic (calcite), rod-like (aragonite) and spherical (vaterite) morphologies. The sizes were confirmed by Transmission Electron Microscopy (TEM) and were found to be between 2–5 µm. The characteristic absorption bands of calcite, aragonite and vaterite were identified using Fourier Transform Infrared Spectroscopy (FT-IR) at 874.41 cm^{-1}, 1022.16 cm^{-1} and 1627.90 cm^{-1}, respectively. The elemental composition of calcium, carbon, and oxygen was confirmed using Energy-Dispersive X-ray (EDX) spectroscopy. The results confirm the potential use of the isolated local soil bacteria as an eco-friendly biological alternative for the bio-concrete industry using the MICP process for construction repair applications, which are expensive and unsustainable.*

[*Citation:* Jamshid, Shireen, F., Khalil, M.S., Habib, F., Yilmaz, S., Aziz, A., Khan, S. (2026). Isolation and characterization of indigenous soil bacteria for sustainable self-healing concrete via microbially induced calcite precipitation. *Bull. Biol. All. Sci. Res.* **11***: 134.* https://doi.org/10.64013/bbasr.v2026i1.134]
Keywords*:* *Microbially Induced Calcite Precipitation; bio-concrete; urease-positive bacteria; Bacillus cereus; calcium carbonate; SEM; self-healing concrete*

Introduction

Concrete is the most widely used construction material across the world, estimated to use up 2–3% of the total energy production of the world and to emit 0.73–0.98 tons of CO_2 per ton of produced cement (Miller et al., 2018). The formation of microcracks is an inevitable result of thermal, mechanical, and chemical stresses in concrete structures and is one of the most common ways in which structural degradation is initiated. Traditional repair methods such as epoxy injection, polysiloxane sealants, and acrylic agents are often costly, environmentally harmful due to their non-biodegradability, and not effectively able to last long (Mignon et al., 2017). To overcome these drawbacks, Microbially Induced Calcite Precipitation (MICP) has become an innovative bio-engineering technology. The enzymatic activity of the bacteria that are urease-positive catalyzes the hydrolysis of urea ($CO(NH_2)_2$) to produce ammonia and carbonate ions (CO_3^{2-}), which combine with calcium ions (Ca^{2+}) to form calcium carbonate ($CaCO_3$). This bio-mineralization process seals microcracks, consolidates porous matrices, and reduces concrete permeability, while concurrently providing structural repair and CO_2 sequestration (Bandyopadhyay et al., 2023). The main biochemical sequence of reactions in the ureolytic pathway of MICP is well known. The enzyme urease breaks down urea into ammonia (NH_3) and carbamic acid (NH_2COOH), which decomposes to yield more ammonia and carbonic acid (H_2CO_3) (Khanjani et al., 2021). *Bacillus, Sporosarcina, Lysinibacillus, Pseudomonas,* and *Staphylococcus spp*. are a few bacterial genera that have exhibited MICP activities. *Bacillus cereus* exhibited high MICP activities due to

its ability to tolerate alkaline pH (9–13), spore-forming ability that allows it to survive for extended periods within cement matrices, and its ability to regularly produce high urease activity in loamy soils (Sohail et al., 2022). Although there is a lot of research on MICP related to various parts of the globe, the bacterial resources of Peshawar, KP, Pakistan were not explored in great detail. The potential of indigenous soil bacteria to have better adaptive characteristics to the local environment, such as alkaline soil pH, moisture level, and nutrient profile, may make them more effective MICP agents. Therefore, in the present study, the urease-positive bacteria were isolated, biochemically characterized, induced to precipitate $CaCO_3$ in vitro, and the precipitates were extensively studied using advanced microscopic and spectroscopic techniques.

Materials and Methods

Study Area

The study was carried out at the Microbiology laboratory of Sarhad Institute of Allied Health Sciences (SUST), Peshawar, Pakistan. Soil sampling was done following aseptic soil collection techniques as per institutional procedures.

Soil Sample Collection

Soil samples were taken from three different agricultural areas of Peshawar, KPK, namely, Peshtakhara Bala (S1), Sarband (S2), and Sangu (S3). Sterilized scoops were used to sample at a depth of 0–15 cm. All samples were placed in sterile, sealed polyethylene bags and sent to the lab.

Physio-Chemical Analysis

Soils were collected, and physio-chemical characterization was carried out at the Agricultural Research Institute, Turnab, Peshawar, following standard methods as outlined by Hameed et al. (2021). The parameters analyzed were pH, soil texture (hydrometer method), moisture content (gravimetric oven-drying at 105°C for 24 h), organic matter (Walkley–Black method) and nutrients (Ca, N, P, K, Mg).

Bacterial Isolation

Each soil sample (1 g) was serially diluted (10-1 to 10-7), and then 0.1 mL of sample was plated on nutrient agar (NA). Plates were placed at 37°C and incubated for 24–48 h. Colonies were isolated and sub-cultured into fresh nutrient agar media plates to isolate them and then were tested for urease activity on Christensen's Urea Agar.

Urease Activity Quantification

The phenol-hypochlorite colorimetric method was used to estimate quantitative urease activity, which is the release of ammonia from hydrolysis of urea. Released ammonia was spectrophotometrically determined at 625 nm after bacterial culture (24 h) was centrifuged (6000 rpm, 10 min), suspended in phosphate buffer (pH 7.0), and incubated with 5 mM urea for 30 minutes at 37°C. Urease activity (U/mL) was defined as the amount of enzyme (in µmol of ammonia released per minute per mL of culture).

Phenotypic and Microscopic Identification

The colony features were documented at 24–48 h on nutrient agar. The Gram staining procedure was carried out using standard protocol.

Biochemical Characterization

Biochemical tests were carried out according to Bergey's Manual of Systematic Bacteriology (Vos et al., 2011)

Molecular Identification (16S rRNA Sequencing)

Genomic DNA of each isolate was isolated using a commercial DNA extraction kit. Universal primers27F (5'-AGAGTTTGATCMTGGCTCAG-3') and 1492R (5'-TACGGYTACCTTGTTACGACTT-3') were used to amplify the 16S rRNA gene (~1500 bp) by PCR. The PCR products were purified and then sequenced at Macrogen Inc., Seoul, Republic of Korea, using the Sanger method. Sequences were retrieved and compared by BLAST analysis (NCBI GenBank) for identification of species. The neighbor-joining method was used for the construction of the phylogenetic tree in MEGA X software, and the bootstrapping was carried out in 1000 replications.

In Vitro $CaCO_3$ Precipitation

The supplemented nutrient broth was made into 3% (w/v) urea and 24 mM $CaCl_2$, and the pH was adjusted to 9.0 before $CaCO_3$ precipitation was induced into the mixture in Eppendorf tubes. Bacterial cultures were inoculated and shaken at 150 rpm, under anaerobic conditions, for 24 hrs. at 37°C. After incubation, the tubes were centrifuged at 8000 rpm for 15 minutes. The supernatant was removed, and the $CaCO_3$ precipitates were washed twice with sterile distilled water, dried at 60°C for 12hrs and stored for characterization.

Precipitate Characterization

Scanning Electron Microscopy (SEM)

Dried precipitate samples were placed on aluminum stubs, and a thin layer of gold-palladium coating was sputtered on the surface to improve the electron conductivity and reduce the charging effect. The crystal morphology, surface topography, and polymorph identification were done by SEM at magnifications of 1000×, 5000×, 10000×, and 30000× (Mengistu & Hordofa, 2026).

Transmission Electron Microscopy (TEM)

In TEM, small amounts of precipitate were deposited on a carbon-coated copper grid, dried under a mercury lamp, and introduced to the TEM chamber. A focused electron beam produced high-resolution images at magnifications of 1000×, 10000×, and 50000× that allowed the precise determination of particle size in the nanometer to micrometer range.

FT-IR Spectroscopy

FT-IR spectra were recorded in the 400–4000 cm^{-1} range with the use of an attenuated total reflectance (ATR) accessory. Dried precipitates were simply placed on the ATR crystal and spectra recorded with 4 cm^{-1} resolution and 32 scans co-added. Peak positions and assignment to specific CO_3^{2-} vibration modes characteristic of polymorphs of calcite,

aragonite and vaterite were identified (Novais et al., 2021).

Energy-Dispersive X-ray (EDX) Spectroscopy

SEM was performed along with EDX to ascertain the elemental composition of the $CaCO_3$ precipitates. Qualitative and semi-quantitative element analysis were performed by qualitative and semi-quantitative analysis of the energy of the characteristic X-rays emitted from the surface of the sample when it was irradiated with an electron beam, using the EDX detector (Jeong et al., 2017).

Statistical Analysis

Each experiment was repeated three times (n = 3). Data were given as mean ± standard deviation (SD). All statistical analyses were done with SPSS version 26.0. The urease activity was determined for significant differences between the isolates by performing one-way ANOVA followed by Tukey's post hoc test with $p < 0.05$ as the cut-off.

Results

Physio-Chemical Analysis of Soil Samples

Table 1 shows the physico-chemical properties of the three soil samples. The pH values of all the areas were found to be alkaline (8.66–8.67), which is typical for the calcareous geology of Peshawar. The soil textures were loamy in S1 and S2 and silt in S3. Moisture content ranged from 29.33% (S3) to 31.51% (S1). The highest percentage of calcium was found at S1 (7.8%) with the isolate with the highest urease activity. The levels of phosphorus and potassium were significantly higher than the minimum levels required for the metabolic activity of bacteria, which indicated nutritionally rich conditions for ureolytic microorganisms.

Table 1. Shows the physio-chemical properties of the three soil samples

S.No.	Parameter	S1 – Peshtakhara Bala	S2 – Sarband	S3 – Sangu
1	pH	8.67 ± 1.00	8.66 ± 0.57	8.66 ± 0.57
2	Soil Texture	Loamy	Loamy	Silt
3	Organic Matter (%)	2.20 ± 0.10	2.31 ± 0.08	2.17 ± 0.06
4	Calcium (%)	7.8 ± 0.10	7.6 ± 0.15	7.2 ± 0.15
5	Nitrogen (%)	0.7 ± 0.20	0.5 ± 0.23	0.5 ± 0.10
6	Phosphorus (%)	13.79 ± 1.54	11.10 ± 1.00	10.46 ± 0.57
7	Potassium (%)	14.79 ± 0.31	12.78 ± 0.58	12.13 ± 1.26
8	Magnesium (%)	11.11 ± 0.99	10.76 ± 1.17	10.12 ± 1.17
9	Moisture Content (%)	31.51 ± 3.53	30.66 ± 3.52	29.33 ± 3.51

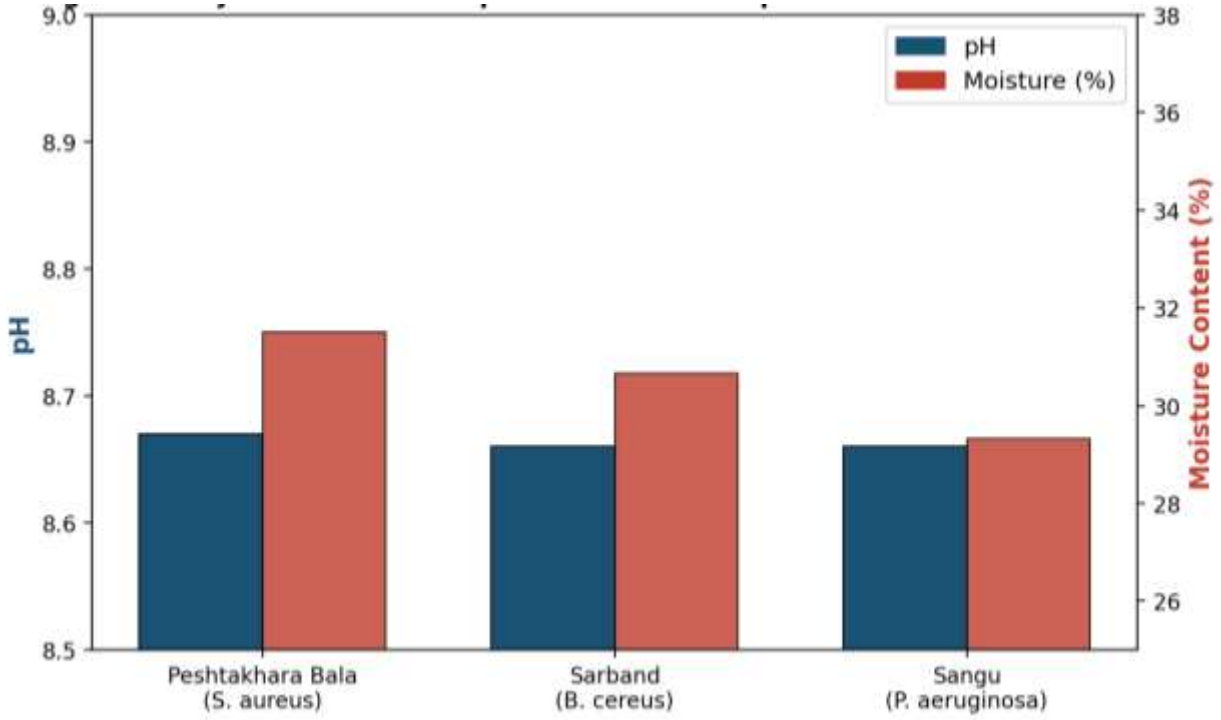

Figure 1. Comparative soil pH and moisture content across the three sampling locations

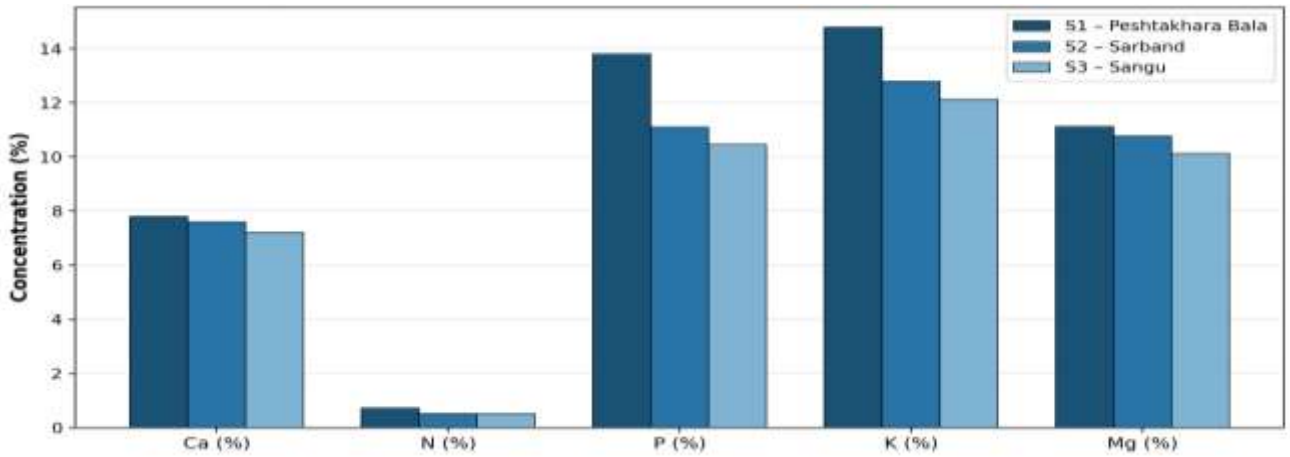

Figure 2. Nutrient composition (Ca, N, P, K, Mg) of the three agricultural soil samples. Peshtakhara Bala consistently demonstrated the highest nutrient concentrations

Isolation and Screening of Urease-Positive Bacteria

A total of 26 bacterial isolates were obtained using nutrient agar by serial dilution plating the three soil samples. On Christensen's Urea Agar slants, 10/26 isolates gave a positive urease reaction (pink) on primary screening. The urease-positive strains were then tested for their capacity for calcite precipitation by supplementing nutrient broth with urea and $CaCl_2$. After centrifugation, the three isolates that produced visible $CaCO_3$ pellets were chosen for full characterization because they had the highest urease activity.

Urease Activity

The urease activity measurements showed that there was a significant difference between the three isolates selected ($p < 0.05$, ANOVA). *Bacillus cereus* had the highest urease activity on Day 4 (580 U/mL); *Pseudomonas aeruginosa* had the highest urease activity on Day 6 (525 U/mL); and *Staphylococcus aureus* had the highest urease activity on Day 6 (515 U/mL). Urease activity was observed to progress in all three isolates, being the fastest escalating in *B. cereus* (Table 2).

Table 2. Urease activity of isolated urease-positive bacteria showing peak activity values, day of maximum activity, and soil source

S.No.	Bacterial Isolate	Day of Peak Activity	Urease Activity (U/mL)	Soil Source
1	*Bacillus cereus*	Day 4	580 U/mL	Sarband (Loamy)
2	*Pseudomonas aeruginosa*	Day 6	525 U/mL	Sangu (Silt)
3	*Staphylococcus aureus*	Day 6	515 U/mL	Peshtakhara Bala (Loamy)

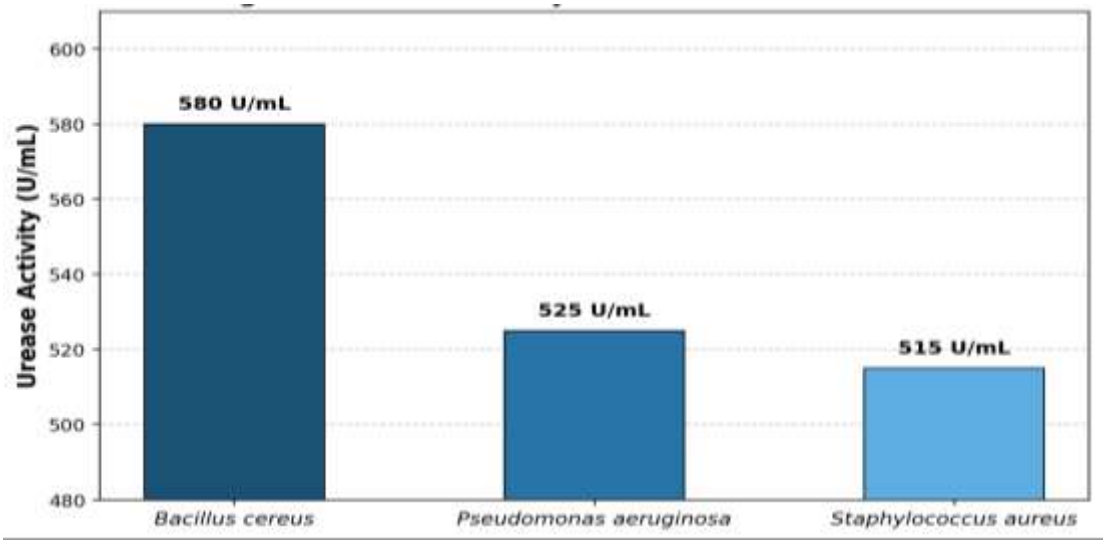

Figure 3. Comparative urease activity (U/mL) of the three isolated bacterial strains. *Bacillus cereus* demonstrated the highest activity at 580 U/mL on Day 4, followed by *Pseudomonas aeruginosa* (525 U/mL) and *Staphylococcus aureus* (515 U/mL)

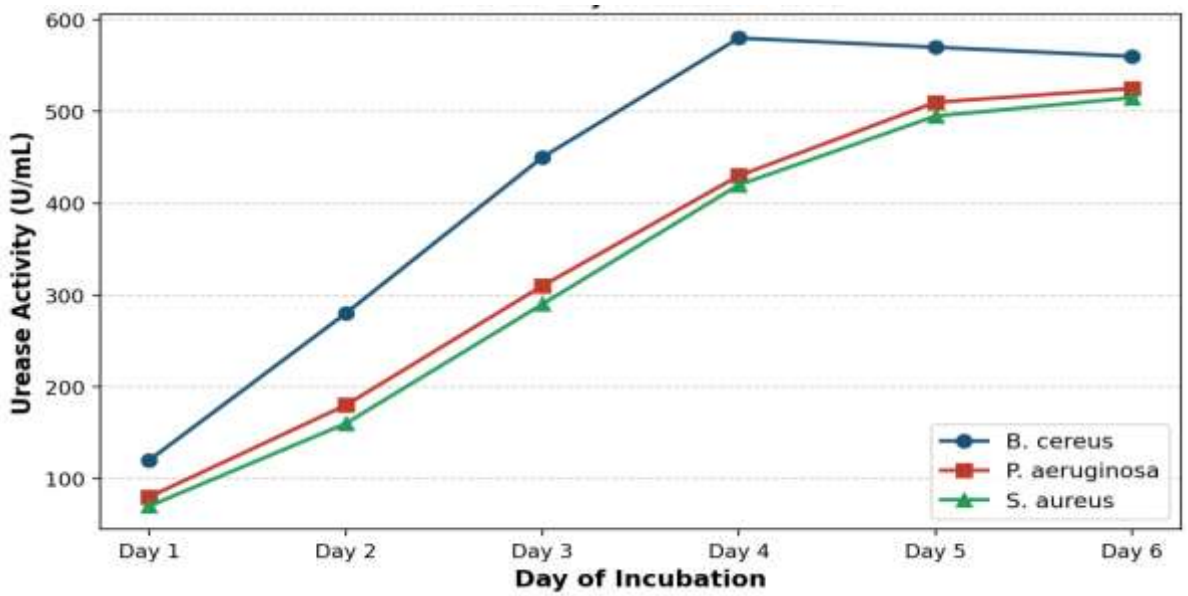

Figure 4. Temporal urease activity profiles of isolated bacterial strains over a six-day incubation period. *Bacillus cereus* shows a steeper early-phase escalation compared to *P. aeruginosa* and *S. aureus*

Phenotypic and Microscopic Identification

Each isolate had a different colony morphology when grown on nutrient agar. *Bacillus cereus* produced large, irregular, opaque, creamy white colonies, which were slightly raised. *P. aeruginosa* colonies made large, circular, pigmented colonies, which were bluish-green, typical of pyocyanin production. *Staphylococcus aureus* colonies were round, smooth, opaque, and golden yellow, which is caused by the pigment staphyloxanthin. Gram staining confirmed: (i) *B. cereus* – Gram-positive (purple), rod-shaped; (ii) *P. aeruginosa* – Gram-negative (pink/red), rod-shaped; (iii) *S. aureus* – Gram-positive (purple), spherical cocci in grape-like clusters. The micro morphological features were similar to those defined by taxonomic descriptions for each species.

Biochemical Characterization

Table 3 shows the full biochemical characteristics of the three isolates. The urease and H_2S production test results were consistently positive and negative, respectively, for all the isolates, while indole and methyl red tests were negative for all. *B. cereus* was catalase-positive, coagulase-negative, and oxidase-negative. *P. aeruginosa* was catalase-negative and showed a positive oxidase reaction, as well as being citrate-positive, reflecting its metabolic versatility. *S. aureus* was catalase-positive, oxidase-positive, and coagulase-positive. These profiles were compared to Bergey's Manual parameters and were in agreement with expected species-level phenotypes.

Table 3. Biochemical characterization and colony morphology of the three calcite-precipitating bacterial isolates

S.No.	Test / Characteristic	*B. cereus*	*P. aeruginosa*	*S. aureus*
1	Colony Morphology	Irregular, opaque, creamy white, raised	Round, opaque, mucoid, bluish-green	Round, smooth, opaque, golden yellow
2	Gram Staining	Gram-positive, rod-shaped, purple	Gram-negative, rod-shaped, pink	Gram-positive, cocci, purple clusters
3	Catalase	Positive (+)	Negative (−)	Positive (+)
4	Oxidase	Negative (−)	Positive (+)	Positive (+)
5	Coagulase	Negative (−)	Negative (−)	Positive (+)
6	Urease	Positive (+)	Positive (+)	Positive (+)
7	H_2S Production	Negative (−)	Negative (−)	Negative (−)
8	Indole Test	Negative (−)	Negative (−)	Negative (−)
9	Methyl Red	Negative (−)	Negative (−)	Negative (−)
10	Citrate Utilization	Negative (−)	Positive (+)	Negative (−)

Molecular Identification (16S rRNA)

16S rRNA gene sequencing and BLAST analysis confirmed species-level identities of all three isolates. For each isolate, sequence similarity values ≥98.5% were found with reference sequences from the NCBI GenBank database: *Bacillus cereus*, *Pseudomonas aeruginosa*, and *Staphylococcus aureus*. Each isolate was analyzed using phylogenetic methods, neighbor-joining, using 1000 bootstrap replicates, which placed each isolate in its genus and species clade, with bootstrap support values >95% at the branch nodes.

In Vitro $CaCO_3$ Precipitation

After 24 h incubation at 37°C, pH 9.0 in supplemented nutrient broth containing 3% urea and 24 mM $CaCl_2$, all three isolates were able to produce visible $CaCO_3$ precipitation. The precipitate pellets were recovered after centrifugation. *B. cereus* produced the highest pellet mass, consistent with its superior urease activity. The high pH of culture broth (up to 9.3) indicated accumulation of ammonium ion and an alkaline micro-environment, which is favorable for biomineralization of $CaCO_3$.

Characterization of $CaCO_3$ Precipitates

Scanning Electron Microscopy (SEM)

The precipitates of $CaCO_3$ were analysed by SEM at different magnifications (1000×–30000×), which showed three different crystal forms of the $CaCO_3$, corresponding with the three major polymorphs of $CaCO_3$, namely (i) irregular crystals with cubic/rhombohedral morphology (calcite), (ii) elongated rod-like structures (aragonite), and (iii) spherical and ellipsoidal crystals (vaterite). Calcite dominated as the main polymorph due to the abundance and regularity of the crystals. Vaterite was found to be smooth spheres, and aragonite was found to have rod-like projections. These observations are in line with the observations made by Gu et al. (2022) and Khanjani et al. (2021).

Figure 5. Schematic Representation of $CaCO_3$Polymorph Morphologies observed by SEM Analysis

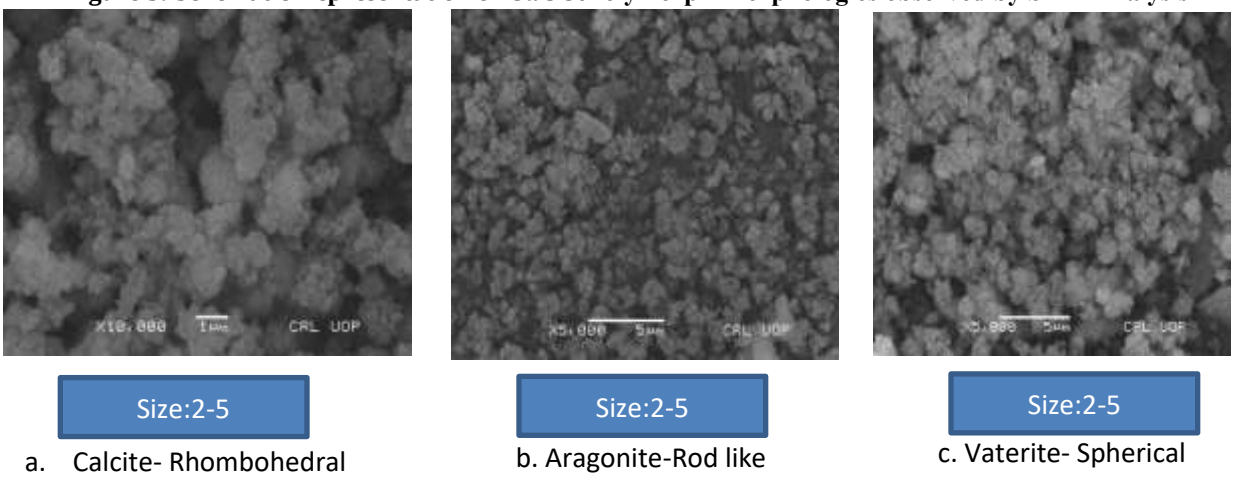

Transmission Electron Microscopy (TEM)

The size of the precipitate particles, as confirmed by TEM analysis, was found to be in the range of 2–5 µm, which is consistent with the results reported in previous studies regarding the size range of the $CaCO_3$ polymorphs produced through MICP (Fan *et al.*, 2023). The size distribution included all three polymorphs that were found: calcite, aragonite, and vaterite, with vaterite particles at the smaller end of size (2-3µm) and calcite crystals at the larger end (4-5µm). In high-resolution TEM at 50000×, the edges of the crystals were seen to be clean, and no amorphous aggregation was seen, which means that the precipitates were well crystallized.

Energy-Dispersive X-ray (EDX) Analysis

The elemental composition of precipitates was confirmed by EDX using peak intensity with a ratio of 1:1:1, which was the stoichiometric ratio of $CaCO_3$. Other minor peaks were found from sodium (Na), chlorine (Cl), phosphorus (P), and silver (Ag), which were from the residual culture media components and the sputter coating of gold and palladium. The peaks appearing in Ca, C, and O are prominent and unambiguously indicate the inorganic carbonate nature of the biogenic precipitate.

FT-IR Spectroscopy

The FT-IR spectroscopy showed that the characteristic CO_3^{2-} vibrational modes were suitable for definitive polymorph identification (Table 4). The 874.41 cm-1 absorption band is an asymmetric CO_3^{2-} stretching band, and the 706.97 cm^{-1} band is an in-plane bending absorption band, which are characteristic of the calcite polymorph. The highest peak at 1022.16 cm^{-1} is due to symmetric stretching in the aragonite lattice. In addition to a broad bending region absorption, there are bands at 1411.21 cm^{-1} and 1627.90 cm^{-1} characteristic of the vaterite polymorph. The presence of both calcite and aragonite signatures as well as vaterite signature of cherty clay, which are present, indicates a polymorphic mixture of biogenic $CaCO_3$, as observed by SEM (Zhao et al., 2023; Ryparova et al., 2021).

Table 4. FT-IR absorption peak positions and polymorph assignments for microbially induced $CaCO_3$ precipitates

Peak (cm^{-1})	Vibration Mode	Polymorph Assignment
706.97	In-plane bending of CO_3^{2-}	Calcite (asymmetric bending)
874.41	Asymmetric stretching of CO_3^{2-}	Calcite (most stable polymorph)

1022.16	Symmetric stretching and bending of CO_3^{2-}	Aragonite lattice structure
1411.21	Stretching vibration of CO_3^{2-}	Vaterite (metastable polymorph)
1627.90	Broad bending region of CO_3^{2-}	Vaterite (unique crystal structure)

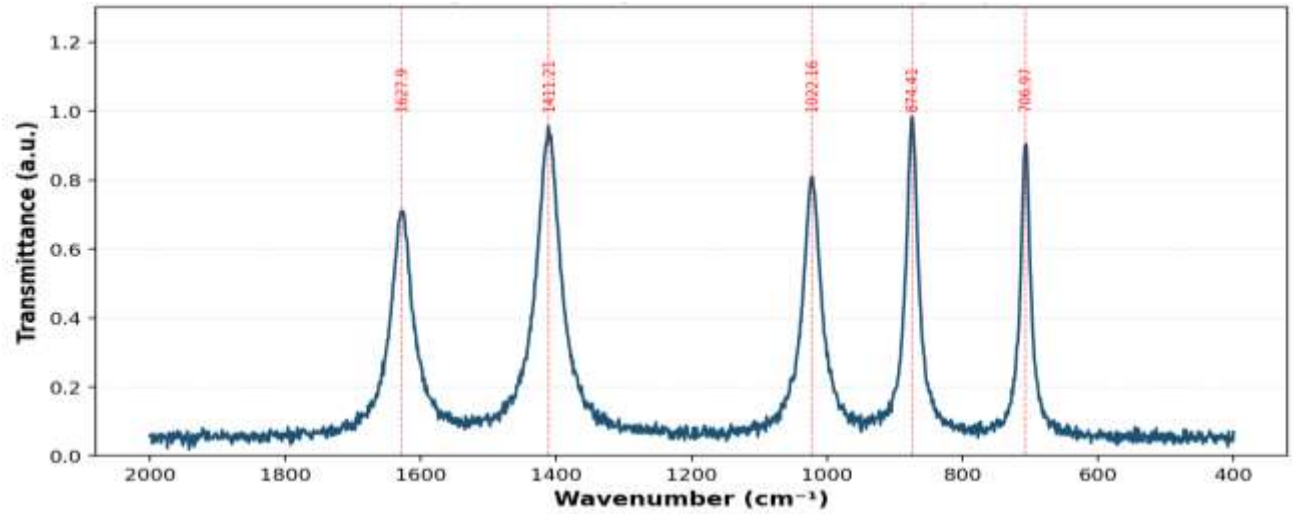

Figure 6. Simulated FT-IR absorbance spectrum of microbially induced $CaCO_3$ precipitates indicating characteristic peaks

Discussion

The present study is the first systematic characterization of urease-positive bacteria capable of MICP from agricultural soils of Peshawar, Khyber Pakhtunkhwa, Pakistan. *Bacillus cereus*, being the highest urease-producing organism (580 U/mL on Day 4) among the local soil isolates, is in line with the reported role of *B. cereus* as a high urease-producing organism in alkaline soils (Sohail et al., 2022; Algaifi et al., 2020). The loamy texture and calcium-rich composition of the Sarband site (soil S2, from which B. cereus was isolated) are consistent with environmental conditions that favor ureolytic metabolic activity and calcite biomineralization. The recent bibliometric study of the international MICP literature (2007–2024) revealed that the only eight publications with Scopus indexing from Pakistan were in comparison to the hundreds of papers from China, India, and the USA (Omoregie et al., 2025). Although the rate of urbanization and concrete durability issues in Pakistan are well documented, microbial resources of Pakistan's agroecosystems have not received much attention and have remained largely uncharacterized for biocementation. To fill this void, the present dataset was obtained from three different types of agricultural soils in the same alkaline basin and serves as a locally relevant alternative to the literature reviewed by Wong et al. (2024) that cataloged mechanisms and field barriers for microbial self-healing concrete, but without local context or South Asian soil resources.

Significantly, the pH for all three sampling sites is in the alkaline range (8.66–8.67). The ureolytic bacteria show maximum urease activity at an alkaline pH (9), whereas the natural alkaline property of soil in Peshawar Basin is pre-adaptative for native ureolytic bacteria in the high pH microenvironment of concrete (pH 12–13) (Algaifi et al., 2020). In the present study, the successful induction of $CaCO_3$ at pH 9.0 in vitro verifies that the ureolytic ability of the strains isolated locally remains unaffected under in vitro conditions relevant to bio-concrete applications. It is notable that P. aeruginosa, an important urease producer, has been recovered. P. aeruginosa is not a frequently cited Pseudomonas species in MICP literature compared to the *Bacillus genus*, however, P. aeruginosa has well-established metabolic versatility, the ability to form biofilms, and an observed tolerance to alkaline environments that make it a possible valuable co-inoculant in MICP mixtures. Although this activity was lower than B. cereus, the urease level was still high (525 U/mL), which should warrant further investigation of the involvement of this species in multi-species bio-concrete formulations. The different polymorphs of $CaCO_3$, as observed in this study, represent the complexity of the biogenic mineralization under the experimental conditions (24mM $CaCl_2$, 3% urea, pH 9.0 at 37 °C). Among the different polymorphs produced, calcite, the thermodynamically most stable, is the most preferred for use in crack-healing applications because of its superior mechanical properties and low solubility (Gu et al., 2022). Vaterite, although metastable, is known to transform to calcite over time, which may yield a prolonged crack-sealing effect. The aspect ratio of aragonite rods is beneficial for interlocking with crack surfaces. It can therefore be helpful to co-precipitate several polymorphs for complete crack filling of different crack geometries.

The particle size of 2-5 µm that was confirmed by TEM is the optimal range to infiltrate into microcracks in concrete (usually less than 0.2 mm = 200 µm). Particles of this size can enter the crack network as a result of capillary action, enter the crack

volume, and crystallize in the cracks to create a dense matrix of interlocked $CaCO_3$ crystals. It has been reported in several in-situ healing tests, such as Algaifi et al. (2020), who obtained total closure of 4 mm cracks after 70 days of treatment with MICP, and Özhan et al. (2023), who obtained healing of cracks up to 0.5 mm after MICP treatment. Contextualizing the findings with existing literature (Table 5) places these findings in the larger context of MICP research. The urease activities in this study (515–580 U/mL) are comparable to or higher than those reported by B. cereus strains isolated from Qatari soils (Sohail et al., 2022), and are close to the activities observed with the laboratory-optimized *S. pasteurii*. Concurrent presence of all three polymorphs of $CaCO_3$ in the same experimental system is less frequently reported and provides granularity in the understanding of MICP under conditions that are closer to South Asian soil chemistry. Two recent studies, both very recent, confirm the importance of considering non-conventional reference strains for identifying indigenous MICP candidates. Shiri et al. (2026) tested over 200 alkaliphiles from extreme environments in Iran using an index of urease and carbonic anhydrase activity, and discovered that several environmental isolates were more efficient at catalyzing the reaction than the urease–carbonic anhydrase complex from the species traditionally considered the "gold standard" for MICP, *Sporosarcina pasteurii*. Also, Mengistu and Hordofa (2026) obtained *Bacillus*, *Lysinibacillus*, and *Halomonas* from soils contaminated with cement in Ethiopia, which produced calcite, vaterite, and trace aragonite in similar proportions as observed in the present study, though the soils were from a chemically more severe environment than the common agricultural soils sampled in this study. Together, these results indicate that high-performing ureolytic strains do not exclusively thrive in extreme or previously investigated environments, and that conventional alkaline agroecosystems (e.g. Peshawar Basin) may be a relatively untapped source of locally adapted bio-concrete strains.

From an environmental perspective, MICP offers a compelling carbon-positive narrative: each mole of $CaCO_3$ precipitated sequesters one mole of CO_2 (as CO_3^{2-}), directly offsetting cement's approximately 0.9 kg CO_2/kg clinker emission factor (Bandyopadhyay et al., 2023). At the construction scale, widespread adoption of MICP bio-concrete could contribute meaningfully to Pakistan's NDC (Nationally Determined Contribution) targets under the Paris Agreement, particularly in the rapidly urbanizing Khyber Pakhtunkhwa region. Translating the present laboratory-scale characterization into field-relevant crack-healing performance will require the kind of quantitative modeling recently demonstrated by Zhou et al. (2026), who applied Box–Lucas and Boltzmann growth models to MICP-treated cracks of varying geometry and reported water-seepage reductions of 70–80% for wide and diagonal cracks, with near-complete (approximately 100%) repair of micro-cracks. Given that the present isolates were characterized only in nutrient-broth microcosms, an analogous modeling framework applied to *B. cereus*- and *P. aeruginosa*-treated mortar specimens would allow the urease activities and polymorph profiles reported here to be related directly to crack-width-dependent healing efficiency, strengthening the case for eventual field deployment. Several limitations of the present study should be acknowledged. First, the in vitro MICP assay does not fully replicate the complex physicochemical environment of a cured concrete matrix, including elevated pH (>12), reduced water activity, and restricted oxygen availability. Future work should assess the survival and MICP performance of these isolates when directly incorporated into cement mortars and concrete specimens. Second, the spore-forming capacity of B. cereus was not quantified, which is critical for longevity assessments. Third, the genetic diversity of the Peshawar soil microbiome may harbor additional high-performance MICP strains not captured by the current isolation protocol; metagenomic approaches are recommended for comprehensive community profiling.

Conclusion

In the present study, three urease-positive MICP-capable bacteria, *Bacillus cereus*, *Pseudomonas aeruginosa*, and *Staphylococcus aureus* were successfully isolated, identified, and characterized from alkaline agricultural soils of Peshawar, Khyber Pakhtunkhwa, Pakistan. Bacillus cereus had the highest urease activity (580 U/mL) and can be considered the most promising bacterium for bio-concrete applications. In vitro biogenic precipitates of CaCO3 were characterized as a polymorphic mixture of calcite, aragonite, and vaterite with a particle size of 2–5 µm, confirmed by TEM, elemental composition verified by EDX, functional group identities confirmed by FT-IR, and crystal morphologies documented by SEM. These results confirm the MICP potential of indigenous Peshawar soil bacteria and provide a scientific foundation for the development of locally sourced, eco-friendly bio-concrete formulations for Pakistan's construction industry. MICP provides a two-fold environmental benefit: crack healing without the use of synthetic chemicals and in situ sequestration of CO_2 as stable mineral $CaCO_3$. Future research should extend beyond laboratory-scale MICP characterization to in-situ concrete incorporation, long-term durability testing, scalability analysis, and techno-economic feasibility assessment for commercial deployment.

References

Algaifi, H. A., Abu Bakar, S., Mohd. Sam, A. R., Ismail, M., Razin Zainal Abidin, A., Shahir, S., & Ali, W. (2020). Insight into the role of microbial calcium carbonate and the factors involved in self-healing concrete. *Construction and Building Materials*, **254**, 119255.

https://doi.org/10.1016/j.conbuildmat.2020.119255

Ariyanti, D., Sasongko, N. A., Fansuri, M. H., Fitriana, E. L., Nugroho, R. A., & Pratiwi, S. A. (2023). Retrofitting of concrete for rigid pavement using bacterial: A metaanalysis. *Science of the Total Environment*, **882**, 166018. https://doi.org/10.1016/j.scitotenv.2023.166018

Bandyopadhyay, A., Saha, A., Ghosh, D., Dam, B., Samanta, A. K., & Dutta, S. (2023). Microbial repairing of concrete & its role in CO_2 sequestration: A critical review. *Beni-Suef University Journal of Basic and Applied Sciences*, **12**(1), 1–10. https://doi.org/10.1186/s43088-023-00344-9

Carter, M. S., Tuttle, M. J., Mancini, J. A., Martineau, R., Hung, C. S., & Gupta, M. K. (2023). Microbially induced calcium carbonate precipitation by *Sporosarcina pasteurii*: A case study in optimizing biological $CaCO_3$ precipitation. *Applied and Environmental Microbiology*, **89**(8), e01794-22. https://doi.org/10.1128/aem.01794-22

Lv, C., Tang, C., Zhu, C., Li, W., Chen, T., Zhao, L., & Pan, X. (2022). Environmental dependence of microbially induced calcium carbonate crystal precipitations: Experimental evidence and insights. *Journal of Geotechnical and Geoenvironmental Engineering*, **148**(7), 04022045. https://doi.org/10.1061/(ASCE)GT.1943-5606.0002821

Davies, R., Teall, O., Pilegis, M., Kanellopoulos, A., Sharma, T., Jefferson, A., & Lark, R. (2018). Large scale application of self-healing concrete: Design, construction, and testing. *Frontiers in Materials*, **5**, 50. https://doi.org/10.3389/fmats.2018.00050

Fan, L., Zheng, J., Peng, S., Xun, Z., & Chen, G. (2023). Experimental investigation on the influence of crack width of asphalt concrete on the repair effect of microbially induced calcite precipitation. *Materials*, **16**(9), 3573. https://doi.org/10.3390/ma16093573

Feng, J., Chen, B., Sun, W., & Wang, Y. (2021). Microbial induced calcium carbonate precipitation study using *Bacillus subtilis* with application to self-healing concrete preparation and characterization. *Construction and Building Materials*, **280**, 122453. https://doi.org/10.1016/j.conbuildmat.2021.122453

Gu, Z., Chen, Q., Wang, L., Niu, S., Zheng, J., Yang, M., & Yan, Y. (2022). Morphological changes of calcium carbonate and mechanical properties of samples during microbially induced carbonate precipitation (MICP). *Materials*, **15**(21), 7752. https://doi.org/10.3390/ma15217752

Hameed, S. M., Hussain, S. A., & Alkhakany, A. J. (2021). Physio-chemical analysis of samples of soil selected from different agriculture areas from Al-Najaf. *Iraqi Journal of Market Research and Consumer Protection*, **13**(2), 125–134.

Iamchaturapatr, J., Piriyakul, K., Ketklin, T., Di Emidio, G., & Petcherdchoo, A. (2021). Sandy soil improvement using MICP-based urease enzymatic acceleration method monitored by real-time system. *Advances in Materials Science and Engineering*, **2021**, 1–12. https://doi.org/10.1155/2021/6620580

Javeed, Y., Goh, Y., Mo, K. H., Yap, S. P., & Leo, B. F. (2024). Microbial self-healing in concrete: A comprehensive exploration of bacterial viability, implementation techniques, and mechanical properties. *Journal of Materials Research and Technology*, **29**, 2376–2395. https://doi.org/10.1016/j.jmrt.2024.01.272

Jeong, J. H., Jo, Y. S., Park, C. S., Kang, C. H., & So, J. S. (2017). Biocementation of concrete pavements using microbially induced calcite precipitation. *Journal of Microbiology and Biotechnology*, **27**(7), 1331–1335. https://doi.org/10.4014/jmb.1702.02058

Jiang, L., Xia, H., Hu, S., Zhao, X., Wang, W., Zhang, Y., & Li, Z. (2024). Crack-healing ability of concrete enhanced by aerobic-anaerobic bacteria and fibers. *Cement and Concrete Research*, **183**, 107582. https://doi.org/10.1016/j.cemconres.2024.107582

Jongvivatsakul, P., Janprasit, K., Nuaklong, P., Pungrasmi, W., & Likitlersuang, S. (2019). Investigation of the crack healing performance in mortar using microbially induced calcium carbonate precipitation (MICP) method. *Construction and Building Materials*, **212**, 737–744. https://doi.org/10.1016/j.conbuildmat.2019.04.035

Joshi, S., Goyal, S., Mukherjee, A., & Reddy, M. S. (2017). Microbial healing of cracks in concrete: A review. *Journal of Industrial Microbiology and Biotechnology*, **44**(11), 1511–1525. https://doi.org/10.1007/s10295-017-1978-0

Khanjani, M., Westenberg, D. J., Kumar, A., & Ma, H. (2021). Tuning polymorphs and morphology of microbially induced calcium carbonate: Controlling factors and underlying mechanisms. *ACS Omega*, **6**(18), 11988–12003. https://doi.org/10.1021/acsomega.1c00626

Khushnood, R. A., Qureshi, Z. A., Shaheen, N., & Ali, S. (2020). Bio-mineralized self-healing recycled aggregate concrete for sustainable infrastructure. *Science of the Total Environment*, **703**, 135007. https://doi.org/10.1016/j.scitotenv.2019.135007

Mengistu, D. M., & Hordofa, D. G. (2026). Isolation and characterization of ureolytic bacteria driving microbially induced calcite precipitation in

cement contaminated soil. *International Microbiology*. https://doi.org/10.1007/s10123-026-00833-0

Mignon, A., Snoeck, D., Dubruel, P., Van Vlierberghe, S., & De Belie, N. (2017). Crack mitigation in concrete: Superabsorbent polymers as key to success? *Materials*, **10**(3), 237. https://doi.org/10.3390/ma10030237

Miller, S. A., Horvath, A., & Monteiro, P. J. M. (2018). Impacts of booming concrete production on water resources worldwide. *Nature Sustainability*, **1**(1), 69–76. https://doi.org/10.1038/s41893-017-0009-5

Novais, Â., & Peixe, L. (2021). Fourier transform infrared spectroscopy (FT-IR) for food and water microbiology. In *Application and Integration of Omics-Powered Diagnostics in Clinical and Public Health Microbiology* (pp. 191–217). Springer.

Oh, S. E., Kim, J. S., Maeng, S. K., Oh, S., & Chung, S. Y. (2024). Influence of bacterial biomineralization conditions on the microstructural characteristics of cement mortar. *Journal of Building Engineering*, **91**, 109455. https://doi.org/10.1016/j.jobe.2024.109455

Omoregie, A. I., Wong, C. S., Rajasekar, A., Ling, J. H., Bousbia Laiche, A., Basri, H. F., Sivakumar, G., & Ouahbi, T. (2025). Bio-based solutions for concrete infrastructure: A review of microbial-induced carbonate precipitation in crack healing. *Buildings*, **15**(7), 1052. https://doi.org/10.3390/buildings15071052

Özhan, H. B., Yildirim, M., Öğüt, H., & Öz, H. G. (2023). Repair of cracks in concrete with the microbial-induced calcite precipitation (MICP) method. *Slovak Journal of Civil Engineering*, **31**(4), 1–8. https://doi.org/10.2478/sjce-2023-0022

Ryparová, P., Prošek, Z., Schreiberová, H., Bílý, P., & Tesárek, P. (2021). The role of bacterially induced calcite precipitation in self-healing of cement paste. *Journal of Building Engineering*, **39**, 102288. https://doi.org/10.1016/j.jobe.2021.102288

Shiri, M., Bahari, A., Khani Sarbangholi, M. M., Ivanovich Vatin, N., Rahmani, H., Ebrahimpour Bozorg, A., Gholamian, E., & Kordlou, M. (2026). Microbial-induced calcite precipitation by indigenous alkaliphilic bacteria: A dual-enzyme strategy for crack-healing in cementitious materials. *Applied Microbiology and Biotechnology*, **110**(1), 93. https://doi.org/10.1007/s00253-026-13764-7

Sohail, M. G., Disi, Z. A., Zouari, N., Nuaimi, N. A., Kahraman, R., Gencturk, B., Rodrigues, D. F., & Yildirim, Y. (2022). Bio self-healing concrete using MICP by an indigenous *Bacillus cereus* strain isolated from Qatari soil. *Construction and Building Materials*, **328**, 126940. https://doi.org/10.1016/j.conbuildmat.2022.126940

Vos, P., Garrity, G., Jones, D., Krieg, N. R., Ludwig, W., Rainey, F. A., Schleifer, K.-H., & Whitman, W. B. (2011). *Bergey's Manual of Systematic Bacteriology: Volume 3: The Firmicutes*. Springer Science & Business Media.

Wong, P. Y., Mal, J., Sandak, A., Luo, L., Jian, J., & Pradhan, N. (2024). Advances in microbial self-healing concrete: A critical review of mechanisms, developments, and future directions. *Science of the Total Environment*, **947**, 174553. https://doi.org/10.1016/j.scitotenv.2024.174553

Zhao, M., Li, S., Wang, M., Guan, X., & Zhao, R. (2023). Adsorption of water and formic acid molecules on the (104) surface of calcite: A theoretical study by DFT-D3. *New Journal of Chemistry*, **47**(18), 8737–8743. https://doi.org/10.1039/D3NJ00378G

Zhou, Y., Li, S., Tabasum, M. H., et al. (2026). Experimental study on self-healing of multiple types of cracks based on microbially induced calcium carbonate precipitation technology. *Innovative Infrastructure Solutions*, **11**, 159. https://doi.org/10.1007/s41062-026-02571-8

Zhu, T., & Dittrich, M. (2016). Carbonate precipitation through microbial activities in natural environment, and their potential in biotechnology: A review. *Frontiers in Bioengineering and Biotechnology*, **4**, 4. https://doi.org/10.3389/fbioe.2016.00004

Statements and Declarations

Funding

The authors declare that they have not received any funds, grants, or other type of financial support for the preparation of this study.

Competing Interests

The authors declare that they have no financial or none, financial competing interests related to this work.

Author Contributions

Conceptualization and study design were performed by Jamshid, FS, MSK and FH. Data collection, bioinformatics analysis, and interpretation were carried out by SY, AA, SK. The writing of the first manuscript draft was done by Jamshid has checked and approved the final version of the manuscript.

Ethics Approval

Since this research does not involve human subjects, animals, or any biological material that would require both the use of and the ethical approval, the authors confirm that no such approval was necessary.

Consent to Participate

Not applicable.

Consent to Publish

Not applicable.

Data Availability

All data generated or analyzed during this study are included in this published article.

Declaration of Generative AI and AI-assisted Technologies in the Writing Process

During the preparation of this work, the author(s) have not used any ChatGPT (OpenAI) tool.